

Effects of Transcranial Direct Current Stimulation on the Motor-Imagery Brain-Computer Interface for Stroke Recovery: An EEG Source-Space study

Vikram Shenoy Handiru*, A. P. Vinod[†], Ang Kai Keng[‡], Effie Chew[§], Cuntai Guan[†]

*Nanyang Institute of Technology in Health and Medicine
Interdisciplinary Graduate School, Nanyang Technological University, Singapore
Email: vikram002@e.ntu.edu.sg

[†] School of Computer Science and Engineering, Nanyang Technological University, Singapore

[‡] Institute for Infocomm Research (I2R), Agency for Science, Technology, and Research (A*STAR), Singapore

[§] National University Health System, Singapore

Abstract—Recently, noninvasive brain stimulation is gaining a lot of attention in stroke rehabilitation. In this paper, we investigate the effects of transcranial direct current stimulation (tDCS) on the motor-imagery brain-computer interface (MI-BCI) performance of stroke patients. To this end, we processed the EEG data collected from a randomized control trial (RCT) study of 19 stroke patients grouped into tDCS and sham. An ensemble method for feature extraction is proposed in this study that combines shrinkage regularized Common Spatial Pattern (CSP) features from sensor-space and sLORETA-based source-space EEG across ten rehabilitation sessions. The classification results of MI vs. Idle state in stroke patients show that the concatenated features from both the sensor- and source space EEG provided an average cross-validation accuracy of 64.5% which is statistically significant ($p < 0.001$) compared to either using source or sensor-space features alone with at least 3% improvement in the accuracy. Further, our findings suggest that the effect of tDCS on the stroke recovery is pronounced in subjects whose delta and alpha band power during the post-tDCS intervention is significantly higher as compared to before intervention. The group-averaged sLORETA activation results showed significantly more number of dipoles activated in the tDCS group as compared to sham. In summary, our study paves a new way to analyze the neural correlates of the MI-BCI performance for stroke rehabilitation.

I. INTRODUCTION

With the advances in Brain-computer interfaces (BCI), it has been demonstrated that the BCI can be used to decode and translate human intentions into control commands [1]. As such, the motor-Imagery (MI) BCI paradigms are extensively explored in healthy as well as stroke subjects with varying types of movement imagination [2], [3]. Although MI-BCI can facilitate the user to modulate his/her sensorimotor rhythms, there are no changes in the cortical excitation. Since the motor recovery is crucial in stroke rehabilitation, the behavioral effects of noninvasive brain stimulation on stroke subjects are studied recently [4], [5], [6], [7] to see if the stimulation alters the motor performance by exciting the motor regions. Most widely known noninvasive brain stimulation methods are transcranial direct current stimulation (tDCS) and transcranial magnetic stimulation (TMS) [4], [6], [8]. Both tDCS and

TMS-based studies conventionally use direct current impulses and magnetic impulses respectively to stimulate certain areas of the brain. In this paper, we study the effects of tDCS on the MI-BCI performance of stroke subjects in a randomized control trial (RCT) setting. Here, the subjects are randomly allocated into two groups: One group received the treatment, whereas another group is considered to be a control group (or sham). In the present context of tDCS intervention for stroke recovery, the group receiving the brain stimulation is called ‘tDCS’ group, and the control group is ‘sham.’ To describe briefly, sham stimulation remains off for the remainder of the stimulation period after emitting a brief current for a very short period (typically, few seconds). When using the sham stimulation, the person does not have the knowledge that they are not receiving prolonged stimulation. Therefore, we can see how much of an effect is caused by the current stimulation as we compare the results in subjects exposed to tDCS to that of subjects exposed to sham. Therefore, we planned to validate the effect of tDCS on the MI-BCI performance by using cortical source EEG features to classify MI and Idle states. Our hypothesis is that the anodal tDCS as an excitatory stimulus will result in better cortical excitation in the motor region, thus facilitating better discrimination between MI and idle state. Our preliminary studies on the healthy subjects have shown that the EEG source space can result in more discriminating features [9], [10] in movement-related tasks. However, there have not been many studies investigating the use of cortical source features in stroke patients. Since the stroke patients have a very limited movement, our goal is to provide useful features that can classify movement intentions with a high accuracy. To this end, we extracted the spatiotemporal features from the sensor space as well as the cortical source space and compared them by evaluating the crossvalidation accuracies across experimental sessions.

In the previous study on the same dataset [7], Ang et.al performed online classification of MI-BCI using Filter Bank Common Spatial Pattern (FBCSP) features based on session-to-session transfer learning. Since this dataset was not studied

from the cortical source perspective, our objective in current work is to investigate the neural correlates of differences between the tDCS and sham group as well as the motor recovery of stroke patients.

To the best of our knowledge, there are no studies which have used source-space EEG features to study the MI-BCI for stroke recovery with tDCS intervention. In this study, we examined the efficacy of MI vs. Idle classification in the tDCS and sham subjects by extracting and classifying source-space EEG features. The remainder of this paper is as follows: Section II describes the Participants, tDCS setup, Experimental procedure, and EEG data acquisition and preprocessing. Section III describes the EEG feature extraction and classification. Section IV exemplifies the results and discussion. Section V concludes this paper.

II. EXPERIMENTAL SETUP

A. Participants

A randomized control trial (RCT) was conducted at National University Hospital (Singapore) in which a total of 42 chronic stroke patients were recruited for this study. Five subjects did not meet the inclusion criteria of at least nine months post stroke onset. Out of the 37 subjects who went BCI screening, 11 subjects did not meet the BCI performance criteria (above chance-level performance), and seven subjects declined to participate further. So, the remaining 19 subjects were randomized into two groups: ‘tDCS’ and ‘sham.’ Fugl-Meyer Assessment (FMA) upper extremity scores of these subjects ranged from 11 to 45 (out of the maximum points of 66). Higher FMA scores indicate better motor functioning. An informed consent from all the subjects was obtained as per the principles of the National Healthcare Group Domain Specific Review Board of Singapore.

B. Transcranial Direct Current Stimulation

The stroke patients in the ‘tDCS’ group were subjected to direct current stimulation for 20 minutes before beginning the MI-BCI experiment. For the ‘sham’ group, the current was applied only for 30 seconds, as it has been reported not to alter the cortical source excitability and also the duration is enough to blinding the subjects from knowing whether they are in the ‘tDCS’ or ‘sham’ group. For specific details of the tDCS procedure, please refer to [7].

C. Experimental Procedure

A total of 10 rehabilitation sessions were conducted over a period of 2 weeks (1st week: 1-5 sessions; 2nd week: 6-10) sessions). Before the rehabilitation session, a calibration session was conducted wherein the EEG data were used to train a model for an online MI-BCI with a robotic feedback [7]. Each rehabilitation session comprised of therapy and evaluation portion wherein the therapy portion had repetitive trials of MI task, and the evaluation portion had randomized order of ‘MI’ and ‘Idle’ tasks. During the ‘MI’ task, subjects were instructed to imagine the movement of their stroke-affected hand toward the target indicated on the 8-point

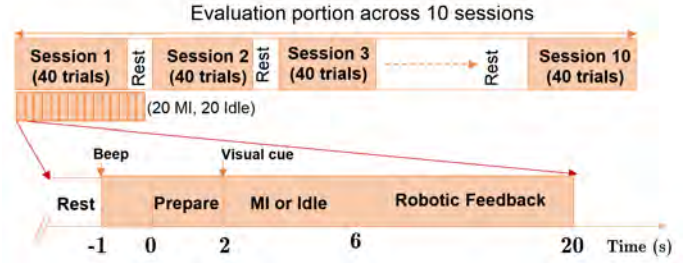


Fig. 1. Experimental timeline of evaluation portion in each MI-BCI rehabilitation session

clock-face game [11] while their affected hand was strapped to the MIT-MANUS robotic exoskeleton, that restricted the volitional movements of the stroke-affected hand. Since the MIT-MANUS robot was programmed to give a feedback based on the output of MI task, subjects were instructed to keep repeating the MI until they saw the visual feedback on whether the trial was successful or a failure. If a trial was correctly classified as MI, then the MANUS robot would move from the center towards a predefined target. In this paper, we used the data from the evaluation portion only as it had trials corresponding to both the classes for evaluating the binary classification. In each session, evaluation portion had 20 trials of ‘MI’ and 20 trials of ‘idle’ task, totaling to 200 trials of each class in 10 sessions per subject. An experimental timeline of an evaluation portion is shown in Fig. 1. After the rest period, a visual cue was shown to indicate the preparation for the trial, after which another visual cue appeared corresponding to a randomized order of MI or Idle task. We used the EEG data from 1s before the stimulus-onset until 3.5s after the onset for the offline analysis.

D. EEG Data Acquisition and Preprocessing

Continuous EEG data were recorded from 27 channels using the Neuroscan Nuamps EEG amplifier. Sampling frequency was 250Hz. EEG trials were bandpass filtered between 0.5-40Hz, followed by common-average referencing. Independent component analysis was performed using an extended infomax algorithm in the EEGLAB toolbox [12], followed by automatic artifact removal using the MARA(Multiple Artifact Removal Algorithm) plugin of EEGLAB [13].

III. METHODOLOGY

A. EEG Source Imaging

The objective of our work is to observe the cortical features in the stroke subjects after tDCS vs. sham intervention. Since the sensor-space EEG do not reveal much information of cortical activity, we propose to employ source localization techniques to study the cortical source space. EEG source imaging comprises of 2 stages: Forward modeling and inverse modeling. Mathematical model of EEG source imaging is expressed as,

$$\Omega = \Theta_f J + \varepsilon \quad (1)$$

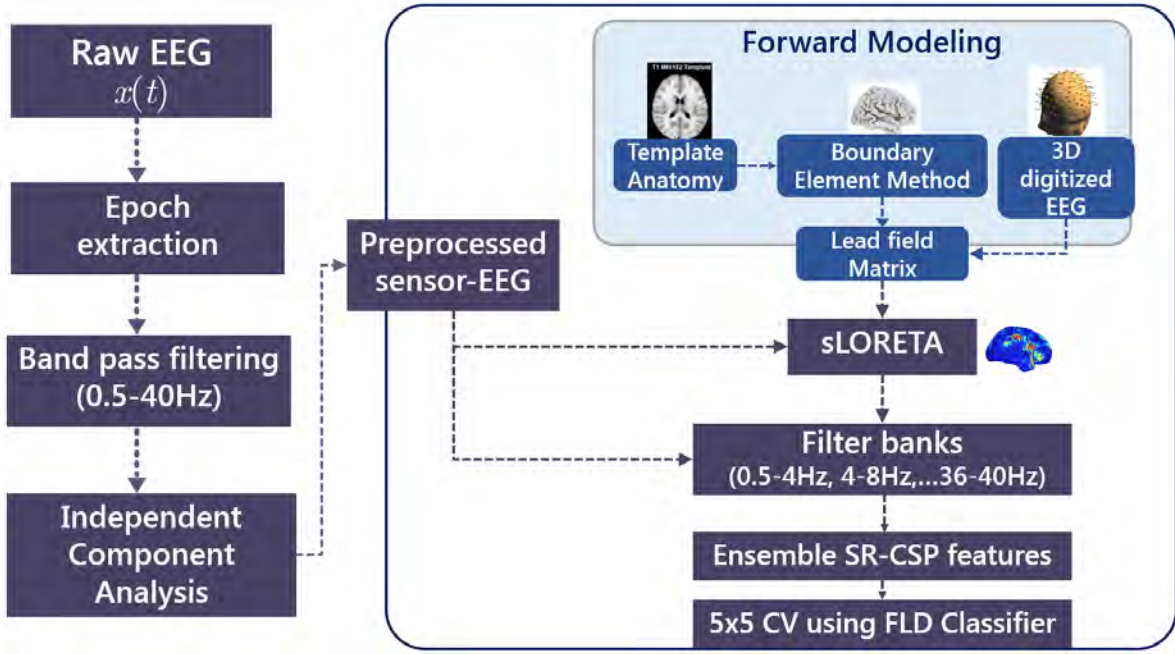


Fig. 2. Overview of the procedural block diagram of EEG data processing in this study.

where, Ω is the scalp EEG recorded from N sensors, Θ_f is the lead field matrix (LFM) of size $N \times m$ (where, $m \gg N$). Θ_f describes the propagation of current from source dipoles (m) to each scalp electrode (N). J is an $m \times t$ matrix of source dipole time series. ε is the noise perturbation matrix with a trial-based noise-covariance matrix computed during the pre-stimulus baseline period. Lead field matrix (Θ_f) is computed during the forward modeling as described below.

1) *Forward Modeling*: A 3 layered shell model is assumed for the forward modeling with the conductivity values of 0.0125 S/m (Skull), 1 S/m (scalp), and 1 S/m (cortex) [14]. Symmetric Boundary Element method (sBEM) in the OpenMEEG toolbox [15] is used to implement the forward modeling that interpolates the triangular meshes to form the head model.

2) *Inverse Modeling*: To get the time series information of source dipoles $J(m, t)$ (where, J is the dipole matrix shown in (1), we need to solve the inverse problem. However, the number of cortical sources (m) obtained modeled using a forward model vastly outnumber the number of scalp electrodes (N), which is an ill-posed problem. Therefore, this under-deterministic problem needs to be solved using the head model and volume conductivity values as a priori information. There are several techniques to solve this inverse problem [16], and we chose standardized Low-Resolution Electromagnetic Tomography (sLORETA) as a nonparametric inverse method [17] which is reported to give a zero-localization error. As a current density estimation method, sLORETA is a regularized variant of minimum norm estimation (MNE) that localizes the sources using the images of standardized current density. At each dipole, the current density value is computed using the

minimum norm estimate as expressed in (2),

$$\hat{J}_{MNE} = \Theta_f^T (\Theta_f \Theta_f^T + \alpha I_N)^{-1} \Omega \quad (2)$$

where, Θ_f is the lead field matrix, and Ω is the scalp EEG as mentioned earlier, I_N is an Identity matrix of size $N \times N$.

B. Dimension Reduction

Since the cortical source-space EEG is of very high dimension ($15002 \text{ voxels} \times 1126 \text{ time samples} \times 20 \text{ trials} \times 2 \text{ classes}$) per session; feature extraction would be computationally prohibitive. Therefore, we use a priori information of regions of interest (ROI) and the state-of-the-art dimensionality reduction method that preserves the local information in a low-dimensional subspace.

1) *Region of Interest (ROI)*: It has been well-established in the literature that the neural population in sensorimotor cortex is responsible for MI and ME tasks. Therefore, we down-sampled the spatial information by picking the voxels that belong to Brodmann Areas BA4 and BA6 that covers the primary motor cortex (M1), premotor cortex, (PMc) and somatosensory cortex areas.

2) *Locality Preserving Projections*: Even after selecting an ROI, the number of voxels belonging to these ROIs was more than 1000. Therefore, we further reduced the number of dimensions to have much more tractable computation in the feature extraction stage. We used Locality Preserving Projection (LPP) as a dimension reduction technique that is insensitive to outliers and other noise as compared to traditional method like Principal Component Analysis [18]. It preserves the neighborhood of data as the nearest neighbor search in a low-dimensional subspace will fetch similar results

to that of high dimensional data [18]. In the current study, the number of reduced dimension is set at 30 which is comparable to the dimensions ($N=27$) of the sensor-space EEG.

C. An Ensemble Feature extraction method using Shrinkage-regularized Filter Bank Common Spatial Patterns (SR-FBCSP)

To evaluate the MI-BCI binary classification performance, we used a regularized version of a popular Common Spatial Pattern (CSP) algorithm, a classical Rayleigh quotient method [19]. Extending the traditional approach of computing CSP using the sensor-space EEG, we propose to use ensemble features by concatenating the features from both sensor, and source space EEG. In principle, CSP maximizes the inter-class (between-class) variance and minimizes the intra-class (or within-class) variance. The objective function of conventional CSP algorithm $J(w)$ is as shown in (3),

$$J(w) = \frac{w^T C_1 w}{w^T C_2 w} \quad (3)$$

where, w denotes the spatial filters, C_i denotes the covariance matrix computed for all the trials belonging to class i . Traditionally, an empirical covariance is used as the covariance matrix. Although it is unbiased and usually works well, it leads to imprecise estimation when the sample size (in this context, number of trials) is small [20]. Therefore, we use the Shrinkage regularized CSP in which a structured estimator (C_c) is used instead of an empirical covariance matrix C_i and it is computed as shown in (4),

$$C_c = (1 - \gamma)C_i + \gamma I \quad (4)$$

where, γ is the shrinkage regularization parameter that has analytical solution [20], I is the identity matrix. As the traditional CSP computation in a single frequency band does not reveal spectral information as much, a filter bank CSP (FBCSP) was proposed in [21]. Based on this approach, we filter the EEG in 10 non-overlapping filter bands ranging from 0.5Hz to 40Hz (0.5-4Hz, 4-8Hz,...,36-40Hz) using a Chebyshev type-II Infinite Impulse Response (IIR) filter with zero-phase. Extending the resultant multiband filtered EEG, we apply SRCSP- now called as SR-FBCSP. It projects the input $X_i(t) = R^{N \times T}$ (N channels $\times T$ time samples in an i^{th} trial) into a spatially filtered subspace Z as, $Z = W \times X$ where the columns of W' corresponds to the spatial filters. In the case of source-space EEG, the input would be $X'_i(t) = R^{N' \times T}$, where N' is the number of low-dimensional cortical sources. The features are computed by log-normalizing the top and bottom ' m ' rows of Z as shown in (5),

$$F_p = \log \left[\frac{\text{var}(\mathbf{Z}_p)}{\sum_{i=1}^{i=2m} \text{var}(\mathbf{Z}_p)} \right] \quad (5)$$

Once these features are computed, we evaluate the classification accuracies using Fishers Linear Discriminant Classifier (FLD). The performance was evaluated in terms of mean classification accuracy using 5×5 cross validation where the data were split into 80% training and 20% testing repeated five times.

IV. RESULTS AND DISCUSSIONS

A. Classification Performance

In this study, we proposed an ensemble feature method that uses spatial features from both sensor and source domain to classify MI vs. Idle state. The plot shown in Fig. 3 illustrates session-wise 5×5 cross validation accuracies of all the subjects across the two groups evaluated using different types of features. In particular, we have evaluated the classification accuracies for each session consisting 40 trials (20 MI, 20 Idle) and performed session-wise 5×5 cross-validation. Subject-specific accuracies for each session is averaged across all the subjects from the same group (tDCS or sham) and is plotted in Fig 3. For both groups (tDCS and sham), the SR-FBCSP features from the sensor and the source space individually were compared with the combined features. In this figure, x-axis indicates the session index (1-10), and y-axis corresponds to percentage classification accuracies averaged over the group of subjects.

The ensemble features resulted in a higher classification accuracy (64.42%) in tDCS group as compared to using either sensor (58.47%) or source space features (61.48%) alone. Similar is the observation in the sham group, although the improvement in the classification accuracy using ensemble features (58.67%) is not significant compared to either sensor (58.04%) or source-space (58.04%) features in sham group subjects. The performance of tDCS group was better than that of sham group. Irrespective of the type of subjects or feature space, there is no clear trend in the classification accuracy over a period of 10 rehabilitation sessions, although the grand-average classification accuracies across different types of features were significantly higher than chance level accuracy. Post-hoc analysis (paired sample t-test) was conducted to observe the efficacy of the proposed method. The ensemble features resulted in a statistically significant ($p < 0.001$) improvement compared to the features from both sensor and source space EEG in the tDCS group, but not in the sham group ($p=0.343$). Similarly, the groupwise comparison revealed that the MI vs. Idle classification accuracies in the tDCS group are significantly higher compared to the sham group ($p < 0.001$).

B. Spectral source power analysis

In addition to the classification accuracy, we also explored the cortical source activation patterns across tDCS and sham groups in different frequency bands. Since we defined an ROI earlier, trial-averaged band power of time series information in these ROIs were computed corresponding to the calibration session that was commenced before the tDCS intervention and the 10th session which is at the end of 2 weeks of tDCS intervention. As a case proof, we studied source-space EEG data of one of the subjects whose MI-BCI classification performance, as well as FMA scores, was improved during the intervention. We found that the average band power of Delta (< 4 Hz) and Alpha (8-12Hz) frequency bands were significantly higher during the post-intervention as compared

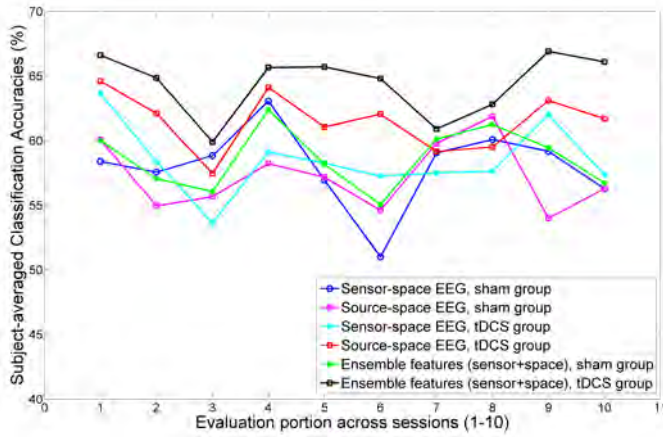


Fig. 3. Group-average session wise 5×5 crossvalidation based binary classification accuracies of MI vs. Idle state using different types of features

to pre-intervention, based on the number of voxels that are significantly different compared to the baseline. The results are shown in Fig. 4 in which the thick line and shaded portion represent the mean and standard deviation of source power of all the dipoles belonging to an ROI determined earlier. Post-hoc two sample t -tests revealed that the tDCS stimulation was associated with significant band power increase ($p < 0.001$) in both delta and alpha frequencies as compared to before the intervention, which concur with the findings in [22].

Extending further, we studied the group-level neural patterns by averaging the source activation across all sessions and subjects in each group. In Fig. 5, we have shown the group-averaged significant source activation based on the paired t -test results at a significance level of 0.05. We found that the number of significant voxels was higher in the tDCS group as compared to the sham group. Interestingly, the significant source dipoles are located in the central region of Brodmann areas BA4 and BA6 which are associated with motor functions. It is to be noted that the subjects received anodal tDCS (or sham) stimulation only in the ipsilesional motor region. Since there were almost equal number of subjects with either right or left-hand stroke-affected, the group average did not reveal any significant cortical excitation in either of the hemispheres. Nevertheless, there is no conclusive causal interpretation of whether the relatively stronger source activation in tDCS group has implications on the MI-BCI performance as well as FMA scores during the therapy.

C. Limitations

As is the case with any BCI study, there is a lot of both intra-subject and inter-subject variability in this study as well. Within each subject, there is a high variability in the MI vs. Idle classification results performance across sessions. Further, both the groups (tDCS and sham) showed a high variability in the session-averaged classification results across subjects. In the previous study [7], the model trained using the calibration session data was transferred to each online session. Although the session-to-session transfer may result in relatively lesser

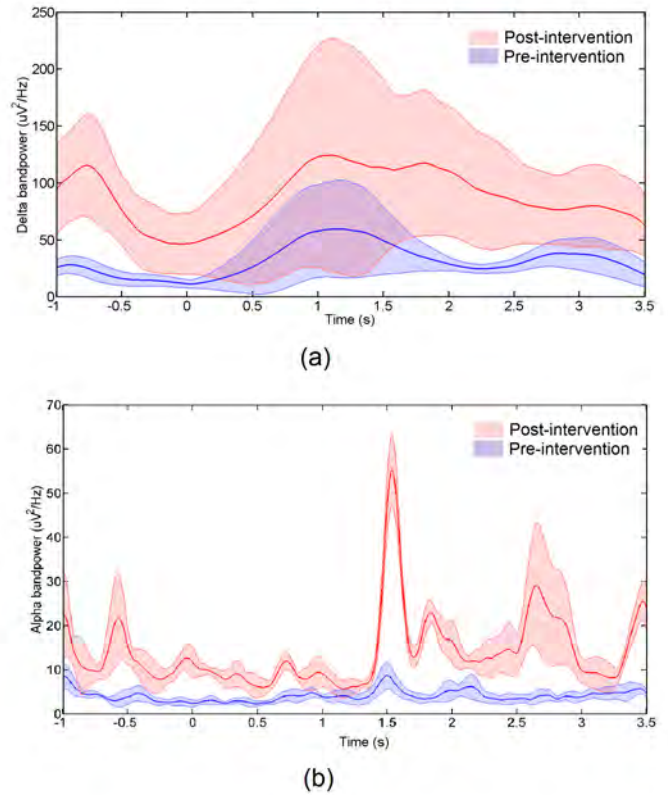


Fig. 4. An illustrative example of comparison between post-tDCS intervention and pre-tDCS intervention spectral source power - (a) delta frequency band (0.5-4Hz) (b) alpha frequency band (8-12Hz). The time-series information corresponds to the source activation in the predefined ROI (BA4 and BA6).

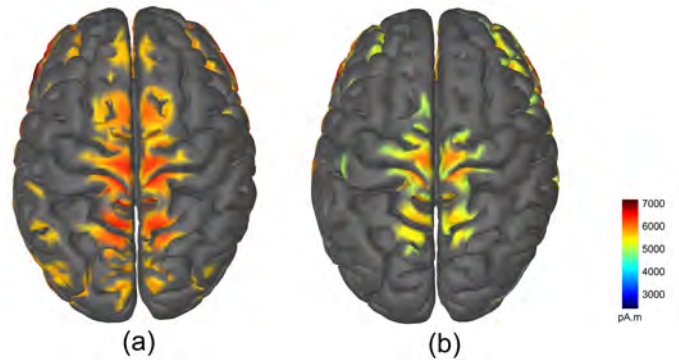


Fig. 5. Group-averaged sLORETA activation results during the MI trials in (a) tDCS and (b) Sham group

variability as compared to cross-validation study, the classification results may not be necessarily better in the case of session-to-session transfer. Since the classification accuracies were computed session-wise, we suspect the training sample size is not enough to obtain good classification accuracies. It would be interesting to investigate robust transfer learning algorithms in the future studies with multiple subjects and sessions.

Also, we have used a subject-independent template anatomy

for the head model digitized based on a fewer number of scalp EEG electrodes which is not ideal for good source localization accuracies. Nonetheless, our study is not as critical from an EEG source localization perspective as is the case with epileptic studies where it is very crucial to achieve a very high localization accuracy of detecting the seizure locations. Further, our study is limited to a relatively fewer subjects and therefore, we need to validate our findings from longitudinal studies in the future. Although we have found that the tDCS-intervention resulted in increase in the bandpower of delta and alpha frequencies in the motor regions, we need to study the causal evidence behind this observation.

V. CONCLUSIONS AND FUTURE WORKS

In this paper, we examined different types of spatial features for classifying MI vs. Idle state in a randomized group of stroke patients receiving noninvasive brain stimulation (tDCS group) and another group receiving a placebo (sham group). We found that an ensemble of features resulting from concatenated spatial features computed using sensor-space and sLORETA-based source EEG gave us higher classification accuracy as compared to using either sensor or source-space features alone. Further, the spectral analysis in the Brodmann Areas BA4 and BA6 showed significant increase in the band power of Delta (<4Hz) and Alpha bands (8-12 Hz) during the tDCS intervention. At the end of 2 weeks of tDCS intervention, the tDCS group showed stronger cortical activation as compared to the sham group.

In our future work, we intend to study the causal interpretation of neural correlates of stroke recovery. The therapy portion of the current dataset is not used for classification as it has only one class (MI) and thus not used for any analysis in this paper. However, the number of MI trials per subject across all the therapy portions of rehabilitation sessions ($N=1600$ trials) will allow us to generalize group-wise causal inference of connectivity measures. Since it has been reported in the literature that the stimulus-based causal interpretation is empirically provable [23], our future work will focus on encoding and decoding of neural correlates corresponding to a given stimulus.

ACKNOWLEDGMENT

The authors would like to thank the BCI team from Institute for Infocomm Research and the clinicians from National University Hospital (Singapore) for providing us the data of stroke patients.

REFERENCES

- [1] J. R. Wolpaw, J. R. Wolpaw, N. Birbaumer, N. Birbaumer, D. J. McFarland, D. J. McFarland, G. Pfurtscheller, G. Pfurtscheller, T. M. Vaughan, and T. M. Vaughan, "Brain-computer interfaces for communication and control." *Clinical neurophysiology*, vol. 113, pp. 767–91, 2002.
- [2] F. Galán, M. R. Baker, K. Alter, and S. N. Baker, "Degraded EEG decoding of wrist movements in absence of kinaesthetic feedback." *Human brain mapping*, vol. 36, pp. 643–654, oct 2014.
- [3] K. K. Ang, K. S. G. Chua, K. S. Phua, C. Wang, Z. Y. Chin, C. W. K. Kuah, W. Low, and C. Guan, "A Randomized Controlled Trial of EEG-Based Motor Imagery Brain-Computer Interface Robotic Rehabilitation for Stroke." *Clinical EEG and neuroscience*, vol. 46, no. 4, pp. 310–20, 2014.
- [4] A. J. Butler, M. Shuster, E. O'Hara, K. Hurley, D. Middlebrooks, and K. Guilkey, "A meta-analysis of the efficacy of anodal transcranial direct current stimulation for upper limb motor recovery in stroke survivors." *Journal of Hand Therapy*, vol. 26, no. 2, pp. 162–171, 2013.
- [5] J. Marquez, P. van Vliet, P. Mcelduff, J. Lagopoulos, and M. Parsons, "Transcranial direct current stimulation (tDCS): Does it have merit in stroke rehabilitation? A systematic review." *International Journal of Stroke*, vol. 10, no. 3, pp. 306–316, 2015.
- [6] A. Saimpont, C. Mercier, F. Malouin, A. Guillot, C. Collet, J. Doyon, and P. L. Jackson, "Anodal transcranial direct current stimulation enhances the effects of motor imagery training in a finger tapping task." *European Journal of Neuroscience*, vol. 43, no. 1, pp. 113–119, 2016.
- [7] K. K. Ang and C. Guan, "BrainComputer Interface for Neurorehabilitation of Upper Limb After Stroke." *Proceedings of the IEEE*, vol. 103, no. 6, pp. 944–953, jun 2015.
- [8] J. Reis, E. Robertson, J. Krakauer, J. Rothwell, L. Marshall, C. Gerloff, E. Wassermann, A. Pascual-Leone, F. Hummel, and P. A. Celnik, "Consensus:Can tDCS and TMS enhance motor learning and memory formation?." *Brain stimulation*, vol. 1, no. 4, p. 363, 2008.
- [9] V. S. Handiru, A. P. Vinod, and C. Guan, "Multi-direction hand movement classification using EEG-based source space analysis," in *2016 38th Annual International Conference of the IEEE Engineering in Medicine and Biology Society (EMBC)*. IEEE, aug 2016, pp. 4551–4554.
- [10] H. Vikram Shenoy, A. P. Vinod, and C. Guan, "A novel supervised locality sensitive Factor analysis to classify voluntary hand movement in multi direction using EEG source space," in *2016 IEEE Intl. Conf. on Systems, Man, and Cybernetics (SMC)*. IEEE, oct 2016, pp. 2795–2800.
- [11] H. I. Krebs, B. T. Volpe, D. Williams, J. Celestino, S. K. Charles, D. Lynch, and N. Hogan, "Robot-aided neurorehabilitation: A robot for wrist rehabilitation," *IEEE Transactions on Neural Systems and Rehabilitation Engineering*, vol. 15, no. 1, pp. 327–335, 2007.
- [12] A. Delorme and S. Makeig, "EEGLAB: An open source toolbox for analysis of single-trial EEG dynamics including independent component analysis," *Journal of Neuroscience Methods*, vol. 134, pp. 9–21, 2004.
- [13] I. Winkler, S. Brandl, F. Horn, E. Waldburger, C. Allefeld, and M. Tangermann, "Robust artifactual independent component classification for BCI practitioners," *Journal of Neural Engineering*, vol. 11, no. 3, p. 035013, jun 2014.
- [14] B. N. Cuffin, D. L. Schomer, J. R. Ives, and H. Blume, "Experimental tests of EEG source localization accuracy in spherical head models." *Clinical neurophysiology*, vol. 112, no. 1, pp. 46–51, jan 2001.
- [15] A. Gramfort, T. Papadopoulos, E. Olivi, and M. Clerc, "OpenMEEG: opensource software for quasistatic bioelectromagnetics." *Biomedical engineering online*, vol. 9, p. 45, 2010.
- [16] R. Grech, T. Cassar, J. Muscat, K. P. Camilleri, S. G. Fabri, M. Zervakis, P. Xanthopoulos, V. Sakkalis, and B. Vanrumste, "Review on solving the inverse problem in EEG source analysis." *Journal of neuroengineering and rehabilitation*, vol. 5, p. 25, jan 2008.
- [17] R. D. Pascual-Marqui, "Standardized low-resolution brain electromagnetic tomography (sLORETA): technical details." pp. 5–12, 2002.
- [18] X. He and P. Niyogi, "Locality preserving projections," *Neural information processing systems*, vol. 16, p. 153, 2004.
- [19] H. Ramoser, J. Müller-Gerking, and G. Pfurtscheller, "Optimal spatial filtering of single trial EEG during imagined hand movement," *IEEE Transactions on Rehabilitation Engineering*, vol. 8, no. 4, pp. 441–446, 2000.
- [20] H. Vikram Shenoy, A. P. Vinod, and C. Guan, "Shrinkage estimator based regularization for EEG motor imagery classification," in *2015 10th International Conference on Information, Communications and Signal Processing (ICICS)*. IEEE, dec 2015, pp. 1–5.
- [21] Kai Keng Ang, Zheng Yang Chin, Haihong Zhang, and Cuntai Guan, "Filter Bank Common Spatial Pattern (FBCSP) in Brain-Computer Interface," in *2008 IEEE International Joint Conference on Neural Networks (IJCNN)*. IEEE, jun 2008, pp. 2390–2397.
- [22] S. R. Soekadar, M. Witkowski, E. G. Cossio, N. Birbaumer, and L. G. Cohen, "Learned EEG-based brain self-regulation of motor-related oscillations during application of transcranial electric brain stimulation: feasibility and limitations," *Frontiers in Behavioral Neuroscience*, vol. 8, p. 93, mar 2014.
- [23] M. Grosse-Wentrup, D. Janzing, M. Siegel, and B. Schölkopf, "Identification of causal relations in neuroimaging data with latent confounders: An instrumental variable approach," *NeuroImage*, vol. 125, pp. 825–833, 2016.